Biochimica et Biophysica Acta, 1101 (1992) 147–153

BBABIO 43681

Molecular reaction mechanism of photosynthetic proteins as determined by FTIR-spectroscopy

Klaus Gerwert

Max-Planck-Institut für Ernährungsphysiologie, Dortmund (Germany)

Key words: Photosynthesis; Membrane protein; Structure-function relationship; FTIR spectroscopy

Introduction

Elucidation of the structure-function relationship in membrane-proteins on a molecular level challenges life-science today. Bacteriorhodopsin and the bacterial photosynthetic reaction-center are the structurally and functionally best characterized membrane-proteins [1,2]. Understanding their mechanism on the molecular level might also give insight into the mechanism of other vectorial proton- and electron-transfer proteins.

In this article a short review of our work on bacteriorhodopsin and photosynthetic reaction centers is given. For more details see referenced publications.

By X-ray and NMR, quiescent ground state structures of proteins on a molecular level are obtained [3,4]. Time-resolved vibrational-spectroscopy provides insight in the dynamics of the intramolecular reactions. Resonance Raman-spectroscopy detects the chromophore-vibrations [5]. FTIR-spectroscopy monitors also protein-sidegroup and backbone-vibrations [6]. In order to select in the IR the small absorbance changes of those groups undergoing reactions from the background absorbance of water and the peptide backbone, difference-spectra between a ground state and an activated state have to be performed [7]. Using time-resolved FTIR techniques, absorbance changes in the order of 10^{-4} beyond a background absorbance of up to 1 between 1800 cm^{-1} and 800 cm^{-1} (i.e., 250 spectral-elements) can be monitored with a time-resolution of up to 25 μs [8,9]. Bacteriorhodopsin and the reaction center are well-suited systems for FTIR-studies. Band assignments derive from use of isotopically labelled proteins or from amino-acid exchange via site-directed mutagenesis [10–12]. Isotopic labelling shifts the frequency of the absorbance band of the labelled groups. Site-directed exchange of an amino acid leads to disappearance of the corresponding absorbance band.

Correspondence to: K. Gerwert, Max-Planck-Institut für Ernährungsphysiologie, Rheinlanddamm 201, 4600 Dortmund 1, Germany.

Bacteriorhodopsin

After light-excitation of bacteriorhodopsin's light-adapted ground-state BR_{570} a photocycle starts with the intermediates J_{610}, K_{590}, L_{550}, M_{410}, N_{530} and O_{640}, distinguished by different absorbance maxima given by the indices. The detailed photocycle is still in dispute (for a recent article, see Ref. 13). Two principal different models are discussed: (i), a linear photocycle with significant back-reactions, especially in the M to BR reaction or (ii), parallel photocycles of different BR-ground-states. During the rise of the M-intermediate a proton is released to the extracellular side, and during the M-decay a proton is taken up from the cytoplasmic side. This creates a proton gradient across the membrane.

The BR to K transition

In Fig. 1, a K-BR difference spectrum is shown. The K intermediate is stabilized at 77 K. Negative bands belong to BR and positive bands to K. The band pattern in the 'fingerprint' region between 1300 cm^{-1} and 1100 cm^{-1} is typical of an all-*trans* to 13-*cis* isomerization [5]. The bands at 958 cm^{-1} and 809 cm^{-1} are caused by retinal Hoop (Hydrogen out of plane) vibrations. They are indicative of a strong distortion of the retinal [5,11]. Comparison with an FT-Raman K-BR difference-spectrum indicates that most of the bands are caused by chromophore-vibrations, especially below 1525 cm^{-1} (Fig. 1) (Gerwert, Hoffmann, Schrader, to be published). This shows that mainly the chromophore is involved in the primary photoreaction. Nevertheless, the difference bands, shifting from 1640 cm^{-1} to 1623 cm^{-1}, and 1546 cm^{-1} to 1533 cm^{-1}, are not observed in the FT-Raman spectrum and must, therefore, be caused by opsin vibrations. Based on their frequency, we assigned them to shifts of the amide-1 (C = O) and amide-2 (NH) vibrations caused

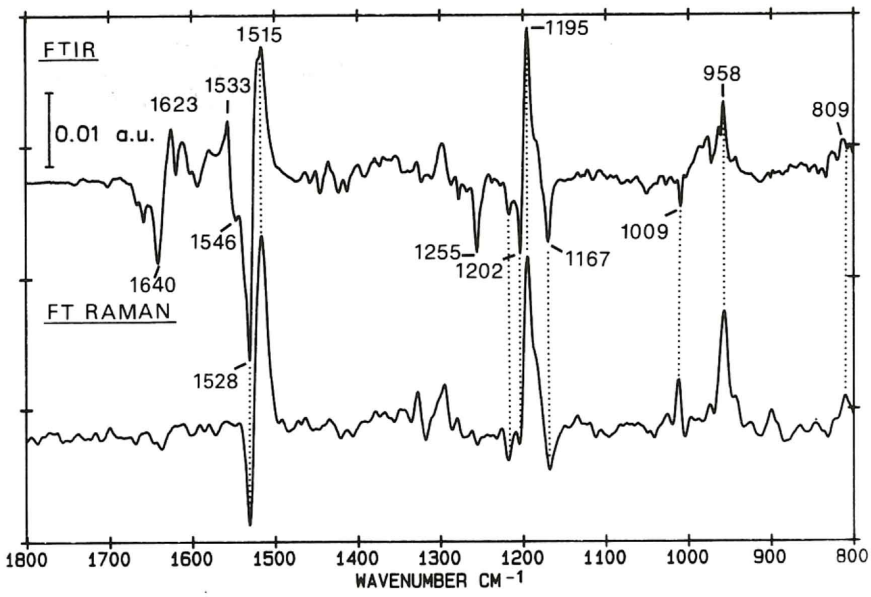

Fig. 1. K-BR difference spectra taken with (a) the FTIR technique and (b) the FT-Raman technique.

by a protein-backbone motion involving two or three residues. The observation of a protein motion already in the primary photoreaction seems surprising. The K-BR difference spectrum indicates that isomerization forces the chromophore and the backbone to drive the reactions.

The reaction $L \rightarrow M \rightarrow N \rightarrow O \rightarrow BR$

The absorbance changes accompanying this reaction pathway can be monitored by the stroboscopic FTIR technique with a time resolution of 20 μs [9]. A 3-D graph of the absorbance changes vs. time is given in Fig 2. Kinetics of specific absorbance changes from Fig. 2

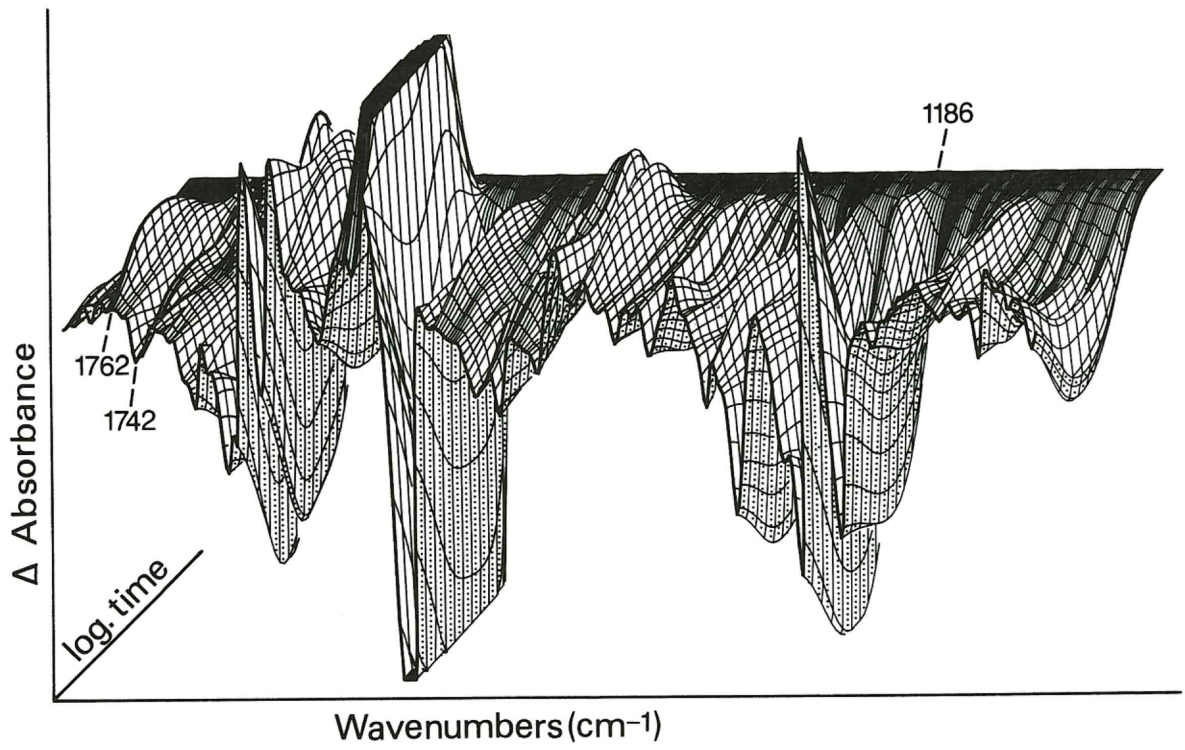

Fig. 2. 3-D graph of the absorbance changes between 1800 cm^{-1} and 1000 cm^{-1} during the bacteriorhodopsin photocycle with 20 μs time resolution. The ethylenic bands at 1525 cm^{-1} and 1550 cm^{-1} are cut to enlarge the other bands.

are given in Figs. 3 and 4. At 1186 cm^{-1} disappearance of the C10–C11 retinal-stretching-vibration can be observed (k_2 and k_5, Fig. 3a) indicating the deprotonation of the Schiff's base in the L to M transition. Its reappearance (k_4) monitors the Schiff base reprotonation in the M to N/O transition. Finally, its time course describes relaxation to the BR groundstate (k_3 and k_6). The deprotonation of the Schiff's base is described by the same apparent rate constants, k_2/k_5, as the protonation of Asp-85 which can be followed at 1765 cm^{-1} (Fig. 3b). From this result we concluded that Asp-85 is the acceptor of the Schiff's base proton on the proton release pathway [8,12]. We proposed, furthermore, that another protonable group must be involved in the proton release pathway. Arg-82 is a likely candidate [29]. Already in 1985 we showed protonation changes of internal aspartic acids [10]. But using site-specific bacteriorhodopsin-mutants allows clear cut assignment of the asp-carbonyl vibrations to specific Asp-side-groups [12]. In Fig 4a, the reappearance of the band at 1186 cm^{-1} is more pronounced, in comparision to Fig 3a, because more N accumulates due to higher pH (pH 8 instead of pH 7). The reprotonation of the Schiff's base is determined by the same apparent rate constant, k_4, as the deprotonation of Asp-96 followed at 1742 cm^{-1} (Fig. 4b). From this, we conclude that Asp-96 is the catalytic proton-binding site on the proton uptake pathway [8,12]. In the structural model Asp-96 is about 10 Å away from the protonated Schiff's base [2]. It might be that much faster proton transfer reactions are involved between Asp-96 and the Schiff's base which are masked. A continuum of absorbance

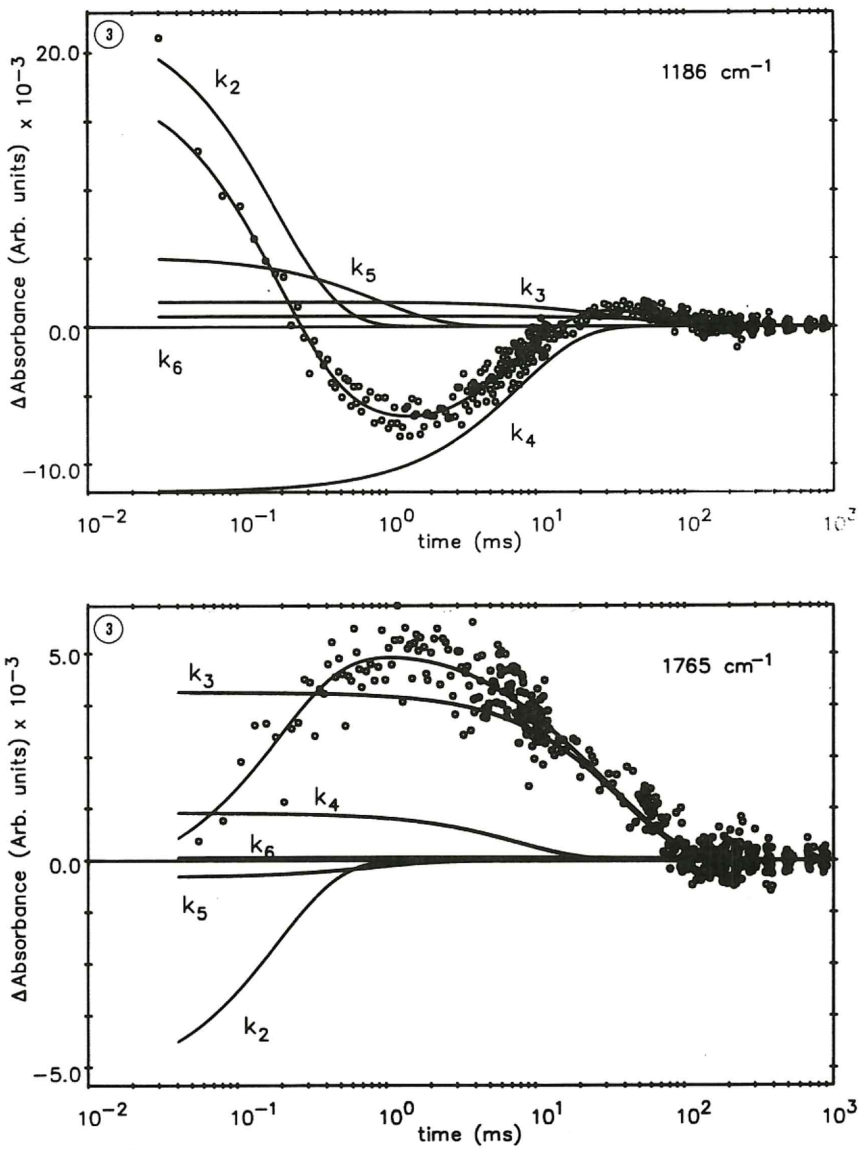

Fig. 3. Absorbance changes at 1186 cm^{-1}, representing de- and reprotonation of the Schiff's base, the central proton-binding site and 1765 cm^{-1}, representing transient protonation of Asp-85. The data, the fitted curve and the apparent rates obtained by exponential-Global-fit analysis are represented. Numbering of the rate-constants represents their appearance in the fit procedure.

decreases above 1760 cm^{-1} may indicate an ice-like proton transfer via an H-bonded network, e.g., via bound water molecules [8,10,12] In principle, only the rate limiting reaction can be resolved by the experiment.

A global fit analysis proves that all reactions in different groups of the protein can be described by the same apparent rate constants [8]. This result implies that the protein works in a synchronized manner like a machine. Nevertheless, decoupling on much faster time scales than 20 μs cannot be excluded.

The assignment of these intramolecular reactions to photocycle intermediates is important. Because significant back-reactions or parallel photocycles have to be considered, we cannot directly deduce natural rate constants describing the photocycle model from apparent ones. Because the number of experimentally accessible apparent rate constants is smaller than the number of natural rate constants, an unequivocal photocycle model cannot be given. Therefore, we used a different approach. The absorbance changes can be described by the following expression:

$$\Delta A(t_i, \nu_j) = \sum_{l=1}^{N} C_{Xl}(t_i)\epsilon_{Xl-BR}(\nu_j) \quad (1)$$

with

$\Delta A(t_i, \nu_j)$ measured absorbance difference relative to the groundstate BR at time t_i at wavenumber ν_j

t_i; i = l, n times where difference-spectra were measured

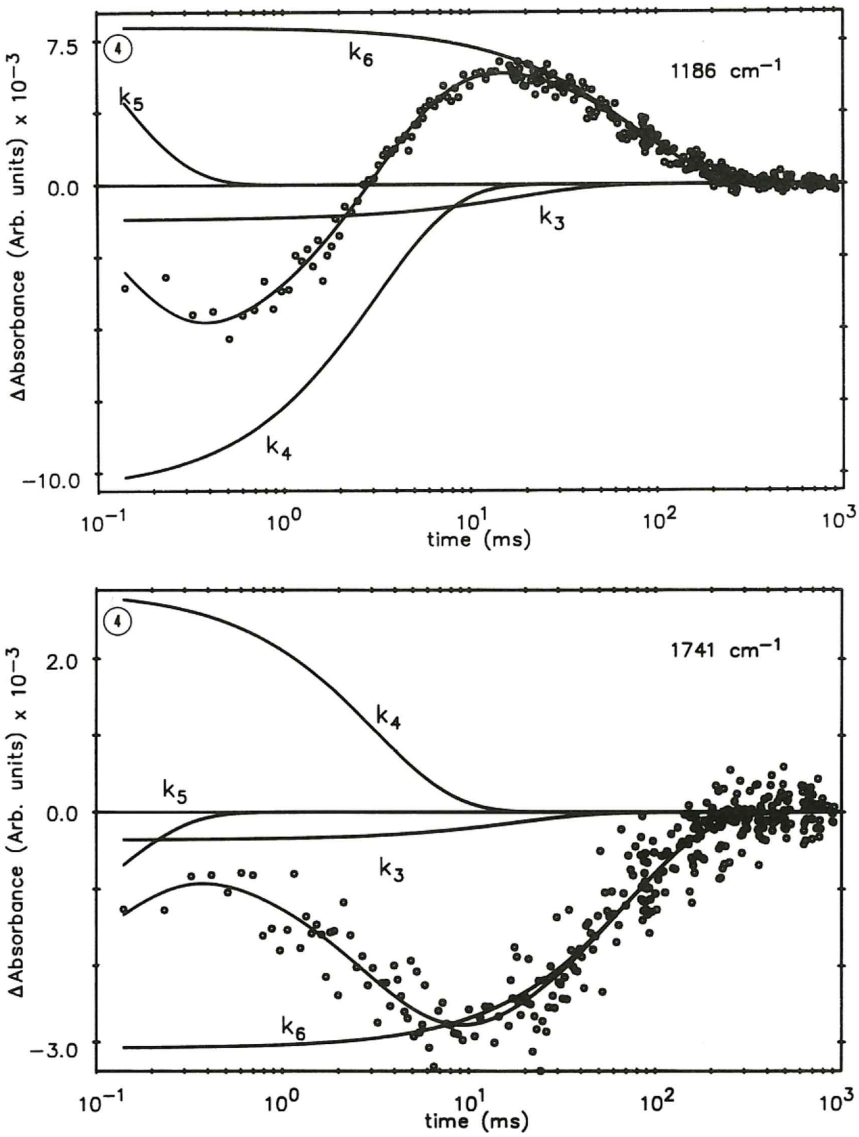

Fig. 4. Absorbance changes at 1186 cm^{-1} representing reprotonation of the Schiff's base and at 1742 cm^{-1} representing transient deprotonation of Asp-96. Data taken at pH 8.

ν_j; j = l, m j-th wavenumber in the spectrum
$c_{Xl}(t_i)$ concentration of intermediate X_i at time t_i
$\epsilon_{Xl-BR}(\nu_j)$ difference of extinction coefficients between intermediate X_i and the ground-state BR at wavenumber ν_j.

In the special case of a model containing the three intermediates M, N and 0, Eqn. 1 has the form

$$\Delta A(t_i, \nu_j) = C_M(t_i)\epsilon_{M-BR}(\nu_j) + C_N(t_i)\epsilon_{N-BR}(\nu_j) + C_O(t_i)\epsilon_{O-BR}(\nu_j) \quad (2)$$

By factor analysis and decomposition we calculated pure intermediate difference spectra ϵ_{x-BR} out of the measured intermediate mixtures (Souvignier, K., Heβling, B., Gerwert, K., to be published). Based on the absorbance changes observed in the calculated pure difference spectra, we can now assign reactions to specific intermediates. The results are summarised in the protonpump-model given in Fig. 5. From the pure difference spectra we conclude that Asp-85 is transiently protonated in the L to M transition and undergoes an environmental change in the M to N transition, which continues in O. Asp-96 is deprotonated in the M to N transition and is already reprotonated in O. The main conformational change of the protein backbone takes place in the M to N transition. We conclude that this conformational change is involved in the orientation of the Schiff's base from the proton release pathway to the proton uptake pathway. This step seems to determine the vectoriality of the pump. Interestingly, blocking the conformational change at low temperature stops the photocyle in M [14,15].

In conclusion, only the chromophore as a switch between the catalytic proton binding sites Asp-85 and Asp-96, and a specific small backbone motion, seem to determine the essential elements of the proton pump. Most of the protein is a quiescent background while functioning.

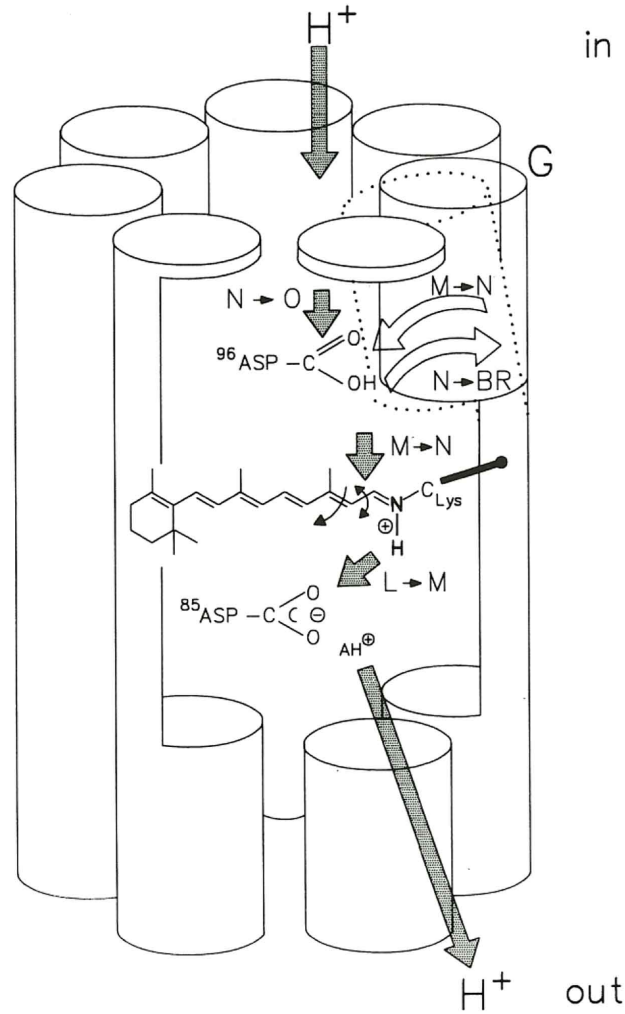

Fig. 5. Proton-pump model of bacteriorhodopsin: After all-*trans*- to 13-*cis*-isomerization and twist around the C14–C15 single bond, the pK of the Schiff's base is reduced and proton transfer from the Schiff's base to Asp-85 in the L to M transition takes place, another group (AH) must be involved in the proton release pathway. In the M to N transition Asp-96 re-protonates the Schiff's base. Thereby, fast proton transfer reactions in an ice-like mechanism may be involved. Asp-96 is reprotonated already in the fast N to O reaction. A conformational backbone change involving two or three residues may be involved in the orientation of the Schiff's base from the proton-acceptor to the proton-donor group. This determines the reset of the pump.

The bacterial photosynthetic reaction center

The FTIR-difference-spectroscopy method is naturally not restricted to bacteriorhodopsin. Recent work has focused on the bacterial photosynthetic reaction centers of *Rhodopseudomonas viridis*. By the FTIR-technique the absorbance changes of the different electron transfer steps beginning at the primary donor P $(Bchl)_2$, going via bacteriopheophytin I (BPh) and the quinone Q_a to the quinone Q_b are monitored [16]. Thereby, the role of the protein environment in the electrontransfer mechanism can be determined. As example, Fig. 6a shows the P^+Q_a-PQ_A difference spectrum of *Rps. viridis*. In order to prevent cytochrome contributions the cytochromes are preoxidized by ferricyanide. The difference spectrum is dominated by the absorbance changes of the primary donor. Bands shifting from 1743 cm^{-1} to 1755 cm^{-1} and from 1672 cm^{-1} to 1712 cm^{-1} are characteristic for oxidation of bacteriochlorophyll *b* in an aprotic environment. They correspond to the absorbance changes of the 10-c-ester- and 9-keto-carbonyl groups of the primary donor [17,18]. The bands at 1477 cm^{-1}, 1439 cm^{-1} and 1392 cm^{-1} represent quinol anion carbonyl vibrations in a protic environment [16,19]. The aprotic environment forces fast re-reduction of the oxidized primary donor which prevents back-reactions. The protic environment stabilizes the reduced quinon state, which is proto-

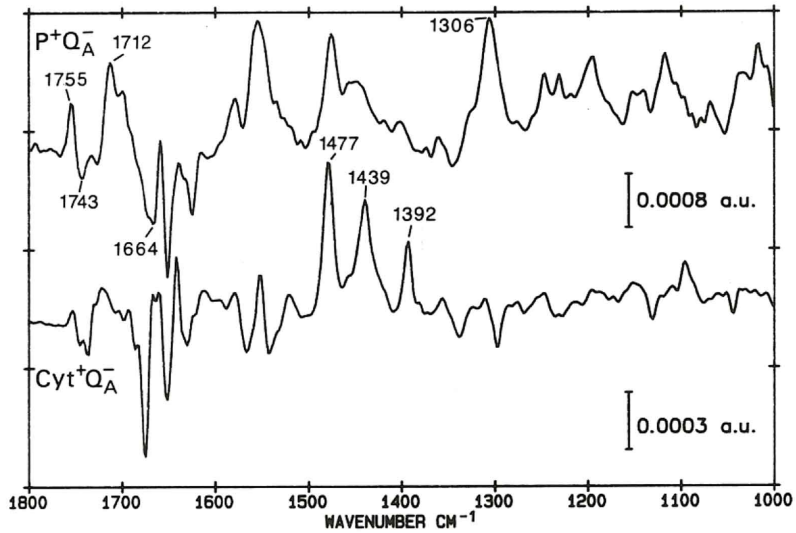

Fig. 6. $P^+ Q_a$-PQ_a and Cyt Q_a-cyt Q_a difference spectra of *Rps. viridis* are shown.

nated relatively slowly. The quinone vibrations are better visualized in the cytochrome + (cyt +) Q_A-difference spectrum (Fig. 6b, Ref. 21). Large-scale structural changes of the protein backbone can be excluded during the electron transfer. Therefore, the charge-separated structures seem to be very close to the quiescent ground state structure [16]. Protein side-group vibrations are not evident. This seems to exclude a major role of side-groups in the electron-transfer mechanism.

Conclusions and Perspectives

In bacteriorhodopsin catalytic proton-binding sites provided by the protein environment are key elements in the proton-transfer mechanism In contrast, in the photosynthetic reaction center, the prosthetic groups are optimally arranged to facilitate fast forward electron transfer reactions; the protein environment seems to serve only as optimized solvent, aprotic at the primary donor and protic at the electron acceptor. It seems that nature uses a mechanical 'switch' in the archaic photosynthetic protein bacteriorhodopsin to serve discrete proton-donor and proton-acceptor groups. But in the evolutionarily more advanced photosynthetic reaction-center, the prosthetic groups are optimally arranged like a wire.

By use of photolabile trigger compounds, such as caged ATP and caged GTP, the presented applications can be extended to non-photobiological systems, such as H^+-ATPase and the GTP-binding ras protein p21.

Acknowledgements

I thank my co-workers Dr. Georg Souvignier, Benedikt Heβling, Johannes le Coutre, Ronald Brudler and Regina Eichas-Nell for engaged and fruitful help, Prof. B. Hess for important support at an early stage, Prof. D. Oesterhelt for providing bacteriorhodopsin mutants and interesting discussions and S. Buchanan and Prof. H. Michel for collaboration with the photosynthetic reaction center. A Heisenberg fellowship and financial support of the Deutsche Forschungsgemeinschaft (Ge 599/7–1) is gratefully acknowledged.

References

1 Deisenhofer, J., Epp, O., Miki. K., Huber, R. and Michel, H. (1985) Nature 318, 618–624.
2 Henderson, R., Baldwin, J.M., Ceska, T.A., Zemlin, F., Beckmann, E. and Downing, K.H. (1990) J. Mol. Biol. 213, 899–929.
3 Schulz, G.E., Schirmer, R.H. (1979) Principles of Protein Structure, pp. 314 S, Springer, New York.
4 Wuetrich, K. (1976) NMR in Biological Research: Peptides and Proteins, Elsevier, New York.
5 Lugtenburg, J., Mathies, R.A., Griffin, R.G. and Herzfeld, J. (1988) Trends Protein Sci. 13, 388–393.
6 Braiman, M.S., and Rothschild, K.J. (1988) Annu. Rev. Biophys. Chem. 17, 541–570.
7 Siebert, F., Mäntele, W. and Gerwert, K. (1983) Eur. J. Biochemistry 136, 119–127.
8 Gerwert, K., Souvignier, G. and Hess, B. (1990) Proc. Natl. Sci. USA. 87, 9774–9778.
9 Souvignier, G., and Gerwert, K. The proton uptake reaction mechanism as determined by stroboscopic FTIR-spectroscopy, submitted.
10 Engelhard, M., Gerwert, K., Hess, B., Kreutz, W. and Siebert, F. (1985) Biochemistry 24, 400–407.
11 Gerwert, K. and Siebert, F. (1986) EMBO J. 5, 805–811.
12 Gerwert, K., Hess, B., Soppa, J. and Oesterhelt, D. (1989) Proc. Natl. Acad. Sci. USA 86, 4943–4947.
13 Váró, G. and Lanyi, L. (1990) Biochemistry 29, 2241–2250.
14 Gerwert, K., Rodriguez-Gonzales, R. and Siebert, F. (1985) in Time resolved Vibrational Spectroscopy (Laubereau, A. and Stockburger, M., eds.), pp. 259–262, Springer, Berlin.
15 Ormos, P. (1991) Proc. Natl. Acad. Sci. USA 88, 473–477.

16 Buchanan S., Michel, H. and Gerwert, K. (1992) Biochemistry 31, 1314–1332.
17 Gerwert, K., Hess, B., Michel, H. and Buchanan, S. (1988) FEBS Lett. 232, 303–307.
18 Mäntele, W.G., Wollenweber, A.M., Nabedryk, E., and Breton, J. (1988) Proc. Natl. Acad. Sci. USA 85, 8468–8472.
19 Breton, J., Thibodeau, D., Berthomieu, C., Mäntele, W., Verméglio, A. and Nabedyk, E. (1991) FEBS Lett. 298, 257–260.
20 Bashford, D., Gerwert, K. (1992) Electrostatic calculations of the pK_a's of ionazable groups in Bacteriorhodopsin. J. Mol. Biol., in press.
21 Nabedryk, E., Berthomieu, C., Verméglio, A. and Breton, J. (1991) FEBS Lett. 293, 53–58